Smart Structures and Systems, *Vol. 28, No. 3 (2021) 319-332*
https://doi.org/10.12989/sss.2021.28.3.319

Finite element simulation and frequency optimization for wireless signal transmission through RC structures

Jingkang Shi [1a], Fei Wang[*2], Dongming Zhang [1b] and Hongwei Huang [1c]

[1] *Department of Geotechnical Engineering, Tongji University, 1239 Siping Road, Shanghai, China*
[2] *Shanghai Institute of Disaster Prevention and Relief, Tongji University, 1239 Siping Road, Shanghai, China*

(*Received July 2, 2020, Revised March 25, 2021, Accepted March 31, 2021*)

Abstract. The enclosed civil structures pose a challenging environment for wireless communication between sensor nodes. Wireless electromagnetic (EM) signal attenuates significantly when transmitting through reinforced concrete structures. This paper simulates the signal attenuation for plain concrete, pure steel rebar lattice and reinforced concrete using finite element method (FEM) in Ansoft High Frequency Structure Simulator (HFSS). Jonscher model is found to be a better concrete dielectric model than Debye model from the attenuation test results. FEM simulation for signal attenuation of reinforced concrete (RC) slab is validated by finite difference time domain (FDTD) simulation and test results from literature. Optimal frequency to minimize the signal attenuation through RC structure is in the range of 0.35 GHz ~ 0.5 GHz. Resonance occurs at $t / (\lambda_c/4) = 2n$ and $t / (\lambda_c/4) = 2n + 1$, $n = 1, 2, 3, 4, \ldots$ for low concrete volumetric water content (VWC). Signal attenuation is highly linear with slab thickness t for high concrete VWC. 433 MHz is suggested for real application of wireless sensor network considering the antenna size and optimization results. FEM simulation is validated by the experiment using intact wireless sensor nodes.

Keywords: finite element simulation; frequency optimization; RC structures; wireless signal transmission

1. Introduction

Wireless sensor network (WSN) is increasingly used in structural health monitoring (SHM) for civil infrastructures such as bridges (Ceylan *et al*. 2013, Jo *et al*. 2013b, Sundaram *et al*. 2013, Flanigan *et al*. 2017), tunnels (Bennett *et al*. 2010, Li *et al*. 2012, Huang *et al*. 2019), utility tunnels (Deng *et al*. 2019, Zhou *et al*. 2020) and buildings (Benatia *et al*. 2014, Raju *et al*. 2015). WSN technique has the advantages of low cost, ease of installation, high sensing fidelity, good scalability and local processing ability (Akyildiz *et al*. 2002, Ou *et al*. 2004). In addition, wireless sensor node makes it possible for self-interrogating structural response data for signs of damage (Lynch 2007, Nagayama *et al*. 2009). WSN is a group of sensor nodes making up a sensor network via wireless communication. Consequently, the effective and reliable communication for sensor nodes is of great importance to the whole monitoring system (Akyildiz *et al*. 2002, Nagayama *et al*. 2007). Specifically, effective communication is vital to the deployment of sensor nodes, network topology design and reliability of monitoring data (Bennett *et al*. 2010, Liu *et al*. 2010, Wu *et al*. 2010).

Civil structures pose a challenging environment for effective wireless communication (Lynch 2007, Liu *et al*. 2009). The large dimensions of civil structures such as bridges and tunnels demands a large wireless communication range. Communication range is largely dependent on signal received strength which is determined by attenuation. Besides, there exists many obstacles such as reinforced concrete walls and floors affecting wireless signal propagation. Building materials including concrete, steel and reinforced concrete can significantly increase packet loss (Linderman *et al*. 2010) and signal attenuation (Lott and Forkel 2001, Micheli *et al*. 2015). For these considerations, a realistic signal propagation model should take account of the signal attenuation of penetrating floors and walls (Biaz *et al*. 2005). Minimization of signal attenuation based on propagation model is helpful to optimize energy consumption and enlarge the reliable communication range due to the limited energy resources (Benatia *et al*. 2014). Received signal strength is highly important for the selection of the optimum topology sensor network for building structures (Haque *et al*. 2015).

Attenuation for RF wave transmitted through concrete slab was calculated by an analytical solution under plane wave assumption (Georgakopoulos and Shan 2010, Jiang and Georgakopoulos 2011). Optimal frequency to minimize the total loss was obtained between 20 ~ 80 MHz both for normal incidence and oblique incidence. Debye model was assumed for frequency dependent concrete dielectric properties in this optimization. Effect of reinforced concrete structures on the Radio Frequency (RF) communication was studied using Finite Difference Time Domain (FDTD) method (Dalke *et al*. 2000). They claimed that maximum transmission occurs when $\lambda_c/2 = t$, $t/2$, $t/4$, $t/8$, …, where λ_c is the wavelength in concrete and t is slab thickness of

*Corresponding author, Associate Professor,
E-mail: wangf@tongji.edu.cn
[a] Ph.D. Student, E-mail: 1710704@tongji.edu.cn
[b] Associate Professor, E-mail: 09zhang@tongji.edu.cn
[c] Professor, E-mail: huanghw@tongji.edu.cn

ISSN: 1738-1584 (Print), 1738-1991 (Online)

reinforced concrete walls. However, concrete permittivity and conductivity were assumed as constants and independent of frequency in this study. Furthermore, only one layer of steel rebar lattice was considered at the middle of reinforced concrete walls, which was not realistic for civil structures. Signal transmission through reinforced concrete slab with two layers of steel rebar was modeled using Finite Element Method (FEM) (Jiang *et al*. 2012). The minimum attenuation was found to occur when $g/(\lambda_0/2) \approx t/(\lambda_c/2) = 1, 2, 3, \ldots$, where λ_0 was the wavelength in free space and g was the steel rebar lattice period. However, optimal frequency was not figured out in this simulation and the adopted concrete dielectric model was also questionable. Jo *et al*. (2013a) studied the penetrated distance of wireless signals into plain concrete in vertical and horizontal directions by laboratory experiment and tested the attenuation of reinforced concrete at 2.4 GHz.

The frequency dependent dielectric properties of concrete are the foundation for analyzing attenuation of signal transmission through reinforced concrete structures. Concrete dielectric properties were generally characterized by Debye model in former studies (Soutsos *et al*. 2001, Sandrolini *et al*. 2007). Debye model considered the mechanism of polarization as Debye response to an applied electric field. Another concrete dielectric model called Jonscher model received increasing attention in recent years. Jonscher model described the polarization mechanism using Jonscher universal dielectric response (Bourdi *et al*. 2008). Jonscher model was believed to be a more realistic model for concrete dielectric properties by the comparison with experimental results (Bourdi *et al*. 2008, Chung *et al*. 2017). However, both models have not been validated in a full signal attenuation test.

This paper aims to model the wireless signal attenuation behavior when transmitting concrete and reinforced concrete structures and explore the optimal frequency range to minimize the signal attenuation. The main work of this paper is simplified to the following aspects. First, Debye model and Jonscher model are incorporated into FE simulation for signal attenuation through plain concrete. FE simulation is validated using attenuation test results and Jonscher model is found to be a better concrete dielectric model. Second, signal transmission through single layer and two layers of steel rebar lattice is simulated and discussed. Resonance phenomenon for two layers of steel rebar lattice for different layer distance is clarified. Third, FE simulation for signal attenuation through RC slab is validated by test results. Optimal frequency for signal attenuation is acquired via the simulation. Effects of concrete VWC, steel rebar lattice period, rebar diameter and slab thickness on optimal frequency are investigated. Signal attenuation for different RC slab thickness and variated concrete VWC is analyzed at 433 MHZ. Finally, FE simulation at 433 MHz is validated by attenuation test using intact wireless sensor nodes.

2. Wireless signal transmission through plain concrete

2.1 Dielectric model of concrete

The electromagnetic properties of concrete are vital to the attenuation of EM signal. As the relative permeability of concrete $\mu_r = 1$, relative complex permittivity of concrete ε_e becomes the key issue. The complex permittivity of a lossy medium is sensitive to the frequency of EM waves. Jonscher model has a good performance in describing the relationship between dielectric constant and frequency for concrete. Jonscher model considers the response due to dielectric relaxation as shown in Eq. (1).

$$\begin{aligned}\varepsilon_e(f) &= \varepsilon_\infty + \chi_r\left(\frac{f}{f_r}\right)^{n-1}\left[1 - i\cot\left(\frac{n\pi}{2}\right)\right] \\ &= \varepsilon_\infty + \chi_e(f)\end{aligned} \tag{1}$$

Where, ε_∞ is the real part of relative permittivity at limiting high-frequency. It is constant and real and describe the mechanism of polarization that rapidly responds to the applied electric field. $\chi_e(f)$ describes the mechanism of dielectric relaxation that responds more slowly to the applied electric field, and the dielectric relaxation is described by Jonscher dielectric response. χ_r and n are fitting parameters to measured experiment results. f is frequency and f_r is the reference frequency.

From Eq. (2), the real and imaginary part of the equivalent complex permittivity $\varepsilon_e(\omega)$ can be derived as shown in Eqs. (2) and (3), respectively. Note that the electrical conductivity of concrete σ is considered in the relative imaginary part in Eq. (3).

$$\varepsilon_e'(f) = \varepsilon_\infty + \chi_r\left(\frac{f}{f_r}\right)^{n-1} \tag{2}$$

$$\varepsilon_e''(f) = \chi_r\left(\frac{f}{f_r}\right)^{n-1}\cot\left(\frac{n\pi}{2}\right) + \frac{\sigma}{2\pi f\varepsilon_0} \tag{3}$$

Another commonly used concrete dielectric model is Debye model. Complex relative permittivity can be expressed as the following equation

$$\varepsilon_e(f) = \varepsilon_\infty + \frac{\varepsilon_{static} - \varepsilon_\infty}{1 + j2\pi f\tau} + \frac{\sigma}{2\pi f\varepsilon_0} \tag{4}$$

where ε_∞ is the permittivity at high frequency, ε_{static} is the permittivity at low frequency, τ is the relaxation time. According to Eq. (4), the real part and imaginary part of relative complex permittivity are expressed using Eqs. (5) and (6), respectively.

$$\varepsilon_e'(f) = \varepsilon_\infty + \frac{\varepsilon_{static} - \varepsilon_\infty}{1 + (2\pi f)^2\tau^2} \tag{5}$$

$$\varepsilon_e''(f) = \frac{(\varepsilon_{static} - \varepsilon_\infty)2\pi f\tau}{1 + (2\pi f)^2\tau^2} + \frac{\sigma}{2\pi f\varepsilon_0} \tag{6}$$

2.2 Finite element simulation for signal attenuation

Wireless signal transmission through plain concrete slab with thickness d is simplified as shown in Fig. 1. Signal is considered as plane EM wave and propagates along the thickness direction of concrete slab. For simplicity, wireless signal is assumed as vertical incidence. Fig. 1 shows the attenuation mechanism of wireless signals transmission through concrete slab. Signal attenuates inside the concrete slab due to absorption and attenuates at the air-concrete interface due to the complex reflection and refraction. ε_e is the relative equivalent permittivity of concrete. ε'_e and ε''_e are the real and imaginary part of ε_e respectively. ε_0 is the permittivity in air, which is equal to permittivity in vacuum.

Wireless signal attenuation by plain concrete slab is determined by frequency and dielectric properties of concrete. Development of analytical solution for the attenuation estimation is very difficult for complex boundaries and inhomogeneous materials such as reinforced concrete (Dehmollaian and Sarabandi 2008). Hence, finite element method (FEM) is adopted to simulate the wireless signal transmission through concrete and reinforced concrete structures in this paper. The commercial software Ansys HFSS has been widely used in the simulation of computational electromagnetic problem (Lin *et al*. 2006, Luo *et al*. 2019). Automatic adaptive mesh generation is used in HFSS, and the simulation precision and reliability are widely acknowledged (Cendes 2016).

Plain concrete slab is modelled as a two-dimension periodic structure to improve the simulation efficiency. HFSS has a unique technique to model such periodic structure as shown in Fig. 2 based on Floquet theorem (Corr 1967, Pathmanathan *et al*. 2011). The excitation for periodic structure is Floquet port at the top and bottom of the model. The distance between the ports and concrete surface should be no smaller than $\lambda/4$, and λ is wavelength of the wireless signal (Jiang 2011). The model side surfaces are set as master and slave boundaries. This kind of boundary regulates that the electric fields have a phase difference between the master surface and slave surface. The floquet port and master-slave boundaries together make it possible to simulate periodic structures in an efficient way.

S parameter is calculated from the finite element model, and S_{21} between port 1 and port 2 is the attenuation in dB for the EM wave transmission through concrete slab. Concrete dielectric properties are input parameters for the simulation, and the response frequency spectrum can be obtained by frequency sweep.

2.3 Experimental study of signal propagation

Experimental investigation of EM signal propagation through different construction materials was carried out by American National Institute of Standards and Technology (NIST). The experiment setup was shown in Fig. 3 (Stone 1997). The measurement system was modified from an ultra-wideband synthetic aperture radar. Two separate transmitting and receiving antennas were directed at each other at a distance of 2 m. The antenna was a kind of dual-polarized Quad-Ridged Horn antenna with a bandwidth of 1.5 GHz between 0.5 GHz and 2.0 GHz. The used antennas

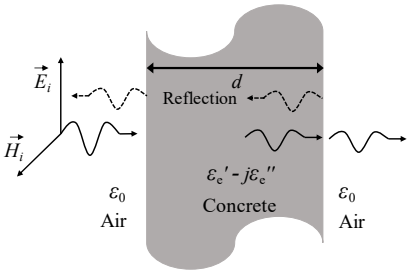

Fig. 1 Wireless signal transmission through plain concrete slab

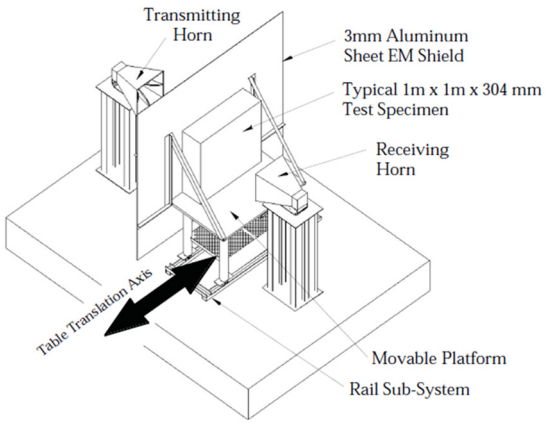

Fig. 3 Experimental setup for EM signal propagation through construction materials (Stone 1997)

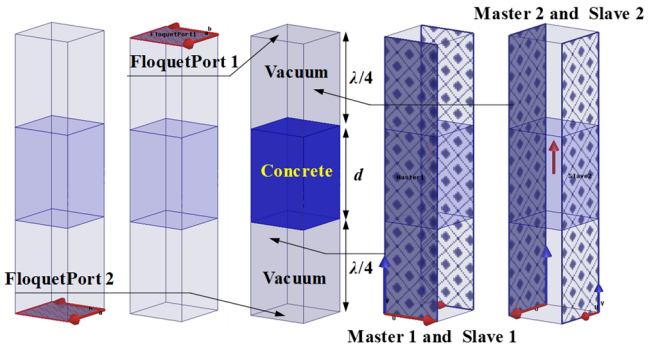

Fig. 2 Modelling of wireless signal transmission through concrete slab in HFSS

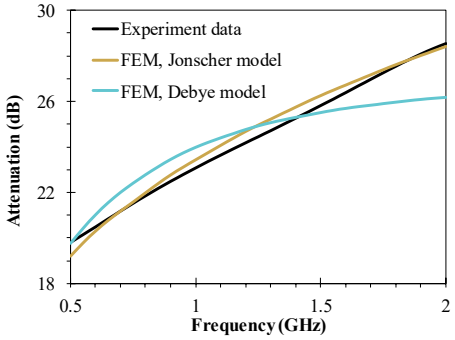

(a) Type 1, thickness 202.3 mm, mean aggregate size 12.7 mm, slump 57 mm, water / cement ratio 0.28

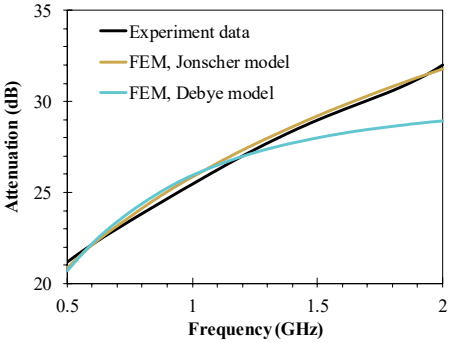

(b) Type 3, thickness 204.1 mm, mean aggregate size 12.7 mm, slump 64 mm, water / cement ratio 0.48

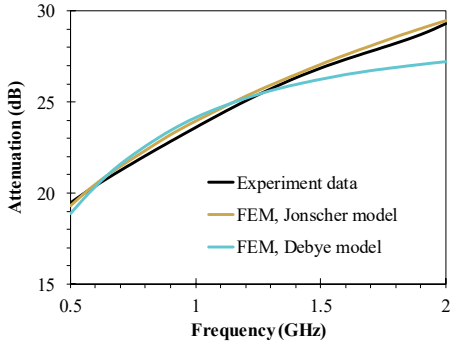

(c) Type 5, thickness 204.0 mm, mean aggregate size 25.4 mm, slump 72 mm, water / cement ratio 0.60

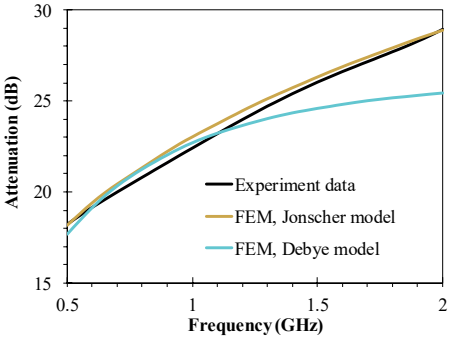

(d) Type 7, thickness 202.0 mm, mean aggregate size 25.4 mm, slump 83 mm, water / cement ratio 0.87

Fig. 4 Comparison between test results and FEM simulation for attenuation of plain concrete

can provide high-gain directional patterns over the bandwidth. Vertical polarization was used for attenuation test to reduce the multipath distortion due to ground bounce. A 3 mm thick aluminum sheet was placed as EM shield to minimize the multipath effect. The magnitude and phase of transmitting and receiving signals were detected by network analyzer.

The protocol for attenuation test consisted of the following three steps: Step 1: Acquire free space response spectra. The free space attenuation was used to divide out the hardware system response. Step 2: Acquire response spectrum for the test specimen. 128 times of measurement were made and the average of 128 samples was recorded at each frequency. Step 3: Spatial variation test. 10 separate tests were performed for each physical specimen. The attenuation spectra could be obtained after post processing.

This paper focused on the wireless signal attenuation through plain concrete, rebar lattice and reinforced concrete. Attenuation test results for different four types of plain concrete are compared with the finite element simulation as shown in Fig. 4. The mentioned two concrete dielectric models are incorporated into the FEM simulation to fit the test results. Four types of concrete specimens with different aggregate size, water/cement ratio and slump are chosen as representatives.

The fitting parameters for the two concrete dielectric models are given in Table 1. From the comparison, it can be seen that FEM simulation with Jonscher model for concrete has a very good agreement with the attenuation test results. The maximum deviation between FEM simulation with Jonscher model and test results is 0.62 dB for Type 1, 0.41 dB for Type 3, 0.39 dB for Type 5 and 0.63 dB for Type 7. However, finite element simulation with Debye model has a poor fitting result especially at higher frequency range. The maximum deviation between FEM simulation with Debye model and test results is 2.38 dB for Type 1, 3.08 dB for Type 3, 2.12 dB for Type 5 and 3.49 dB for Type 7. Hence, Jonscher model is a better dielectric model in characterizing frequency dependent concrete permittivity.

Table 1 Fitting parameters of dielectric models in the attenuation test of concrete specimens

Concrete specimen	Debye model				Jonscher model			
	ε_∞	ε_{static}	τ	σ	ε_∞	χ_r	n	σ
Type 1	6.00	9.20	0.35×10^{-9}	0.107	5.97	6.3	0.32	0.045
Type 3	5.70	9.30	0.33×10^{-9}	0.11	5.67	7.4	0.30	0.035
Type 5	5.50	9.10	0.32×10^{-9}	0.92	5.50	6.9	0.30	0.027
Type 7	5.10	8.90	0.35×10^{-9}	0.076	5.17	7.2	0.30	0.010

3. Wireless signal transmission through reinforced concrete structure

3.1 Signal transmission through rebar lattice

Reinforced concrete structure is a composite of concrete and steel rebar. Steel rebar is a completely different material

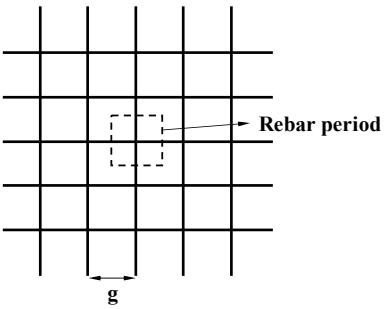

(a) Layout of steel rebar lattice

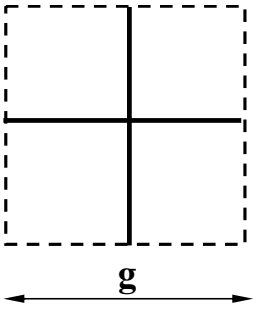

(b) A periodic unit of rebar lattice in simulation

Fig. 5 Periodic simulation of steel rebar lattice

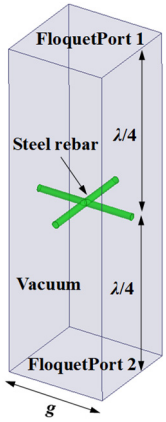

(a) Single layer

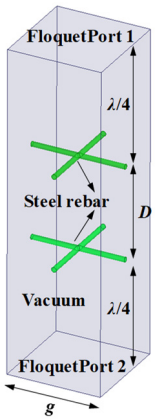

(b) Two layers

Fig. 6 Modelling of steel rebar in HFSS with Floquet mode

compared to concrete due to its high conductivity. EM signals almost cannot transmit into the steel rebar and are considered fully reflected at the air-steel interface. The steel rebar in two perpendicular directions makes up a lattice as shown in Fig. 5(a). The main parameters of the lattice are the period g and rebar diameter d. A periodic unit is modelled as shown in Fig. 5(b) based on Floquet theorem.

Fig. 6 shows the periodic modelling of steel rebar lattice in HFSS. Material of steel rebar is simulated as steel stainless and the conductivity is 1100000 S/m. The surface of rebar is set to perfect E boundary. It ensures that there is no electromagnetic field inside steel rebar and the wave is all reflected at rebar surface. There are usually two layers of rebar inside the reinforced concrete structure, so this paper talks about the single layer shown in Fig. 6(a) and two layers of rebar shown in Fig. 6(b).

Attenuation test for single layer of steel rebar was conducted in the mentioned laboratory experiment. The rebar diameter is 19 mm, and two kinds of rebar period g = 140 mm and g = 70 mm were considered in the test. The comparison between FEM simulation and test results for EM signal attenuation is made in Fig. 7. FEM has a good agreement with test result in higher frequency range while FEM has a deviation from the test result in lower frequency band. The maximum deviation is 7.1 dB at 0.5 GHz for g = 70 mm and 4.6 dB for g = 140 mm. The trend that attenuation increases with the decrease of frequency is validated by test results.

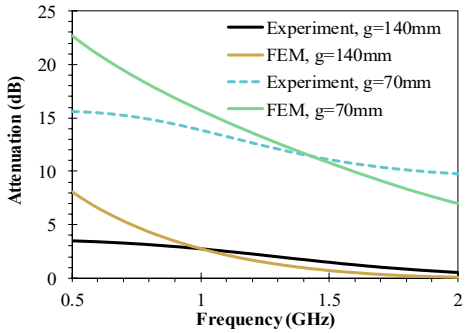

Fig. 7 Comparison between test results and FEM simulation for attenuation of single layer rebar lattice

Attenuation of signal transmitting through single layer steel rebar at different rebar lattice periods is shown in Fig. 8(a). Rebar diameter is 10 mm to decrease the effect on signal attenuation in this discussion. Signal wavelength λ and rebar lattice period g are coupled together to determine the attenuation. The indicator of g/λ is used to measure the lattice size relative to wavelength λ. Signal attenuation L_p is smaller than 2 dB if $g/\lambda > 0.5$, which means 80% of signal power has been transmitted through rebar lattice. Signal frequency should be as high as possible to minimize attenuation for given lattice period.

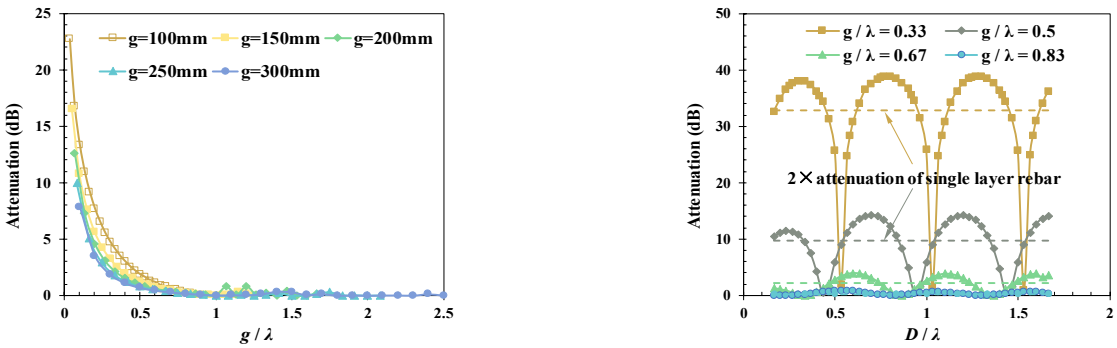

(a) single layer of steel rebar, d = 10 mm (b) two layers of steel rebar, d = 32 mm

Fig. 8 Signal attenuation through steel rebar lattice

Signal attenuation through two layers of steel rebar lattice is investigated in Fig. 8(b). In the simulation, f = 1 GHz and λ = 300 mm. Steel rebar diameter is 32 mm as the unfavorable condition for signal transmission. Apart from rebar lattice period g/λ, distance between two layers of steel rebar D/λ is also influencing to signal attenuation. EM waves resonate between the two layers of steel rebar lattice. The signal attenuation of two layers is not equal to two times of single layer. Resonance occurs at $D/(\lambda/4) = 2n$, n = 1, 2, 3, … and this resonance weakens the signal attenuation of two layers of lattice. Another resonance occurs at $D/(\lambda/4) \approx 2n - 1$, n = 1, 2, 3, …, and this resonance strengthens the signal attenuation. Resonant amplitude is affected by lattice period g/λ. Amplitude is defined as half of the difference between maximum and minimum attenuation. The amplitude is 18.0 dB for g/λ = 0.33 and decreases to 6.8 dB for g/λ = 0.5. Resonance has very little effect on signal attenuation when lattice period g/λ exceeds 0.5 because the attenuation of single layer is already smaller than 2 dB.

3.2 Validation of HFSS model for reinforced concrete structure simulation

As shown in Fig. 9(a), reinforced concrete slab is generally composed of two layers of steel rebar lattice with period g and plain concrete with thickness t. The concrete cover layer on steel rebar is 50 mm thick. The signal attenuation by reinforced concrete slab is composed of absorption by concrete and scattering by two layers of steel rebar lattice. Different from transmission through pure rebar lattice, signal wavelength will be reduced by concrete. Wavelength change in concrete will exert a significant effect of signal attenuation as the influencing values of g/λ and D/λ are increased. Signal transmission through reinforced concrete slab is modelled using finite element method as shown in Fig. 9(b). A periodic part with size g is modelled in HFSS based on Floquet theorem.

Finite element simulation in HFSS is compared with simulation results of FDTD obtained by Dalke *et al*. (2000) as shown in Fig. 10. The simulated reinforced concrete slab has only one layer of steel rebar lattice in the middle. The layout parameters are slab thickness t, lattice period g and steel rebar diameter d. Concrete dielectric property was independent of frequency with conductivity σ = 1.95 mS/m and relative dielectric constant ε_r = 6. Signal attenuation for two kinds of reinforced concrete slab at the frequency range of 0.1 ~ 2.5 GHz are compared in Fig. 10. Root Mean Square Error (RMSE) of the simulated attenuation between FEM and FDTD is 2.6 dB, and maximum difference is 8.0 dB for g = 76.2 mm, d = 19.1 mm, t = 152.4 mm shown in Fig. 10(a). RMSE is 1.7 dB and maximum difference is 4.3 dB for g = 76.2 mm, d = 19.1 mm, t = 203.2 mm shown in Fig. 10(b). The comparison result shows FEM simulation have a very good agreement with FDTD simulation.

The FEM simulation for signal transmission through reinforced concrete slab is compared with test results in

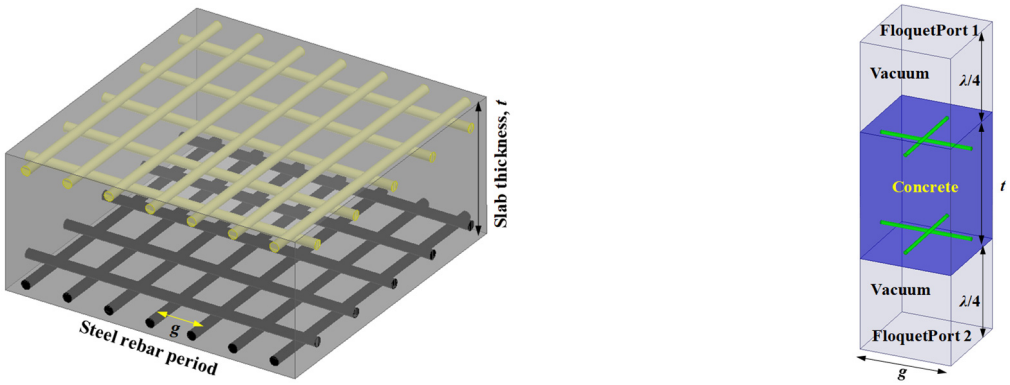

(a) Layout of reinforced concrete slab (b) Periodic simulation in HFSS

Fig. 9 Finite element modelling of reinforced concrete slab

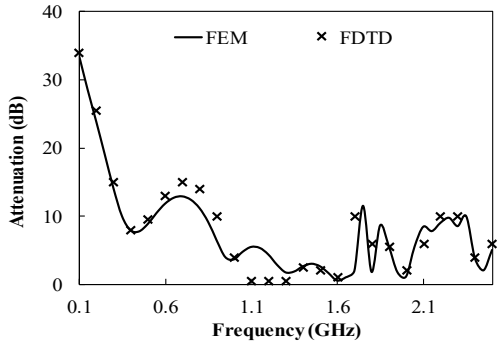

(a) g = 76.2 mm, d = 19.1 mm, t = 152.4 mm

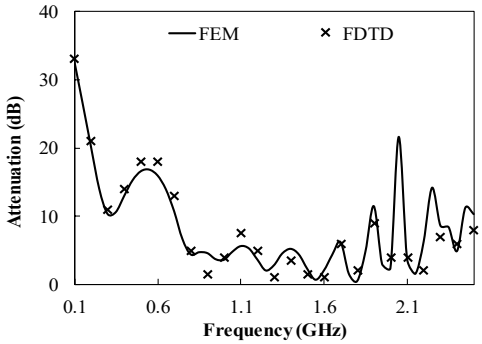

(b) g = 76.2 mm, d = 19.1 mm, t = 203.2 mm

Fig. 10 Simulation result comparison between FEM and FDTD for signal transmission through reinforced concrete slab

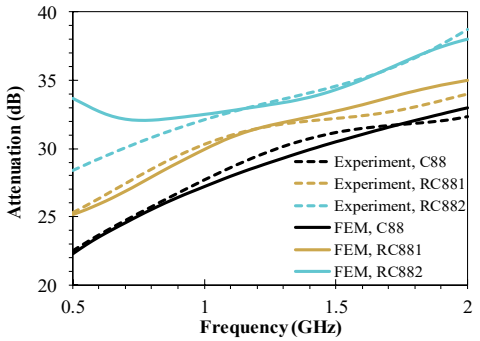

Fig. 11 Comparison between test results and FEM simulation for attenuation of reinforced concrete specimens

Fig. 11. The steel rebar lattice in the reinforced concrete is the same as pure rebar lattice discussed in Part 3.1. Rebar period is 140 mm for specimen RC881 and 70 mm for RC882. C88 is plain concrete specimen with thickness of 203 mm. The Jonscher model is used to fit the test results in the FEM simulation. The fitted parameters for C88 are as follows: n = 0.29, χ_r = 7.8, ε_∞ = 6.5, σ = 0.045. The maximum deviation is 0.84 dB, which shows a good agreement between test results and FEM simulation. Then the obtained parameters for Jonscher model are used to simulate the attenuation for reinforced concrete specimen RC881 and RC882. The maximum deviation is 1.17 dB for RC881 and 5.29 dB for RC882. It can be seen that the deviation for RC882 mainly lies at the lower frequency band. It shows that the error comes from the deviation of steel rebar simulation. Overall, the FEM simulation in HFSS has an acceptable accuracy for EM signal attenuation analysis.

Table 2 Fitted parameters of Jonscher model for concrete samples with different VWC

VWC	n	χ_r	ε_∞	f_r/GHz
h_1 = 0.2%	0.80	0.60	4.11	0.1
h_2 = 2.8%	0.74	1.49	4.45	0.1
h_3 = 5.5%	0.74	3.87	3.75	0.1
h_4 = 6.2%	0.60	2.99	4.94	0.1
h_5 = 9.3%	0.54	4.77	5.75	0.1
h_6 = 12.0%	0.62	7.49	4.39	0.1

3.3 Frequency dependent dielectric properties of concrete

The dielectric constants of concrete have been tested by many laboratory experiments. A widely acknowledged result for concrete samples with different VWC is considered in this paper (Soutsos *et al*. 2001), and the fitted parameters of Jonscher model are given in Table 2 (Bourdi *et al*. 2008).

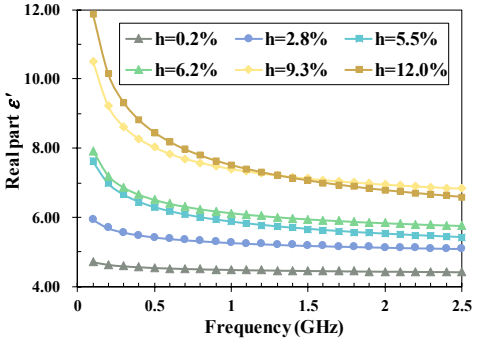

(a) Real part

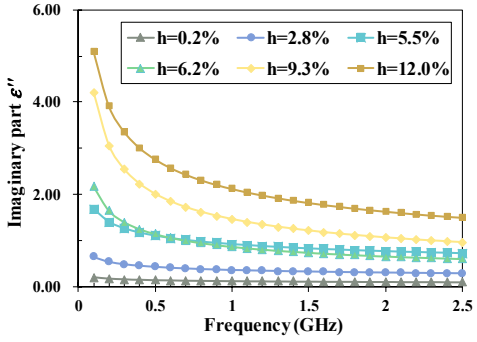

(b) Imaginary part

Fig. 12 The relative equivalent permittivity of concrete vs. frequency

According to Jonscher model, the relationship between the relative equivalent permittivity of concrete and frequency is plotted in Fig. 12. It can be seen that both the real part and the imaginary part are decreasing with the increase of frequency. The real part is gradually converged to ε_∞ as the increase of frequency. Concrete VWC has a significant effect on the real part in 0.1-2.5 GHz frequency range. The real part of the relative permittivity increases with the increase of VWC. The tendency of imaginary part with the increase of frequency and VWC is the same with that of real part. The imaginary part is converged to 0 with the increase of frequency. Jonscher model implies that frequency has a significant effect on of concrete dielectric constant which is crucial to wireless signal transmission through reinforced concrete structure.

3.4 Frequency optimization for signal transmission through reinforced concrete

Since the attenuation of signal transmission through reinforced concrete structure is highly frequency dependent, it is of great value to explore the optimal frequency range to minimize the attenuation. From what has been discussed above, signal attenuation for plain concrete increases with the increase of frequency while attenuation for steel rebar lattice decreases with the increase of frequency. Consequently, it is very likely that an optimal frequency exists for signal transmission through reinforced concrete slab. Concrete VWC, steel rebar lattice period g, rebar diameter d and slab thickness t are all influential factors to signal attenuation as discussed. The effect on these factors on the optimal frequency will be discussed in the following passages.

Effect of concrete VWC on signal attenuation is investigated in Fig. 13. Slab thickness is 350 mm, rebar diameter is 10 mm and rebar lattice period is 100 mm in this simulation. There exists an optimal frequency $f_{optimal}$ which minimizes the attenuation for signal transmission through reinforced concrete slab. Signal attenuation decreases with the increase of frequency before $f_{optimal}$. Concrete VWC has little influence on the total attenuation at this stage, and attenuation caused by rebar lattice is predominant. Attenuation increases with the increase of frequency if frequency exceeds $f_{optimal}$. The optimal frequency is influenced by concrete VWC, and $f_{optimal}$ = 0.5 GHz for h_1 = 0.2 %, $f_{optimal}$ = 0.45 GHz for h_1 = 2.8 %, $f_{optimal}$ = 0.42 GHz for h_3 = 5.5 % and h_4 = 6.2%, $f_{optimal}$ = 0.4 GHz for h_5 = 9.3 %, $f_{optimal}$ = 0.35 GHz for h_6 = 12 %. The optimal frequency is in the range of 0.35~0.5 GHz for different concrete VWC. The minimized attenuation $L_{p,min}$ is 2.0 dB for h_1 , 4.7 dB for h_2, 9.8 dB for h_3, 10.0 dB for h_4, 14.3 dB for h_5 and 17.5 dB for h_6 at each optimal frequency.

Effect of steel rebar lattice period g on signal attenuation through reinforced concrete slab is studied in Fig. 14. In this discussion, the related parameters are as follows: concrete VWC h_5 = 9.3%, rebar diameter d = 10 mm, slab thickness t = 350 mm. Similar trends for the attenuation in 0.1 ~ 2.5 GHz frequency range can be seen from Fig. 14. Optimal frequency $f_{optimal}$ exists for different lattice period g. $f_{optimal}$ = 0.4 GHz for g = 100 mm, $f_{optimal}$ = 0.35 GHz for g = 120 mm, $f_{optimal}$ = 0.33 GHz for g = 140 mm, $f_{optimal}$ = 0.31 GHz for g = 160 mm, $f_{optimal}$ = 0.3 GHz for g = 180 mm. Optimal frequency lies in the range of 0.3~0.4 GHz for different g. With increase of lattice period g, effect of steel rebar is weakened and it behaves more like a plain concrete slab. This leads to the decrease of $f_{optimal}$ with the increase of g. Rebar lattice period has little influence on the minimum signal attenuation as $L_{p,min}$ is in the range of 10.7 ~ 14.3 dB. This is caused by the reduction of signal wavelength in concrete and increase of g/λ_c. In the frequency range of 0.1 ~ 2.5 GHz, g/λ_c will easily arrive the boundary of 0.5 as discussed in the pure rebar lattice attenuation. So, rebar lattice period has limited influence on signal attenuation through reinforced concrete slab at $g \geq 100$ mm.

Effect of rebar diameter on signal attenuation is illustrated in Fig. 15. Simulation parameters are as follows: slab thickness t = 350 mm, concrete VWC h_5 = 9.3%, lattice period g = 100 mm. g is set as 100 mm because effect of rebar diameter will naturally decrease with the increase of g value. Optimal frequency $f_{optimal}$ lies in the range of 0.4 ~ 0.45 GHz with variated rebar diameter d, and $f_{optimal}$ slightly increases with the enlargement of d. The minimum attenuation $L_{p,min}$ at $f_{optimal}$ is increasing with the enlargement of d. $L_{p,min}$ increases from 15.1 dB at d = 12 mm to 24.8 dB at d = 28 mm. This phenomenon is also related to value of g/λ_c. Rebar diameter has little effect on signal attenuation for pure rebar lattice if g/λ exceeds 0.5. Therefore, rebar diameter has very limited effect on both optimal frequency and minimum attenuation for signal transmission through reinforced concrete slab.

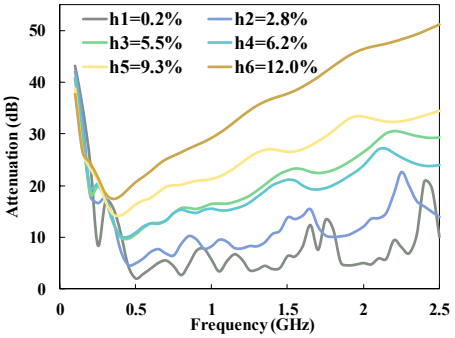

Fig. 13 Effect of concrete VWC on the signal attenuation

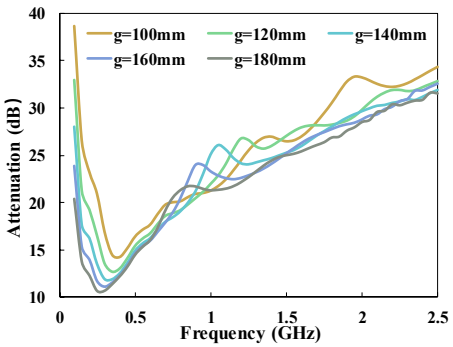

Fig. 14 Effect of rebar period on the signal attenuation

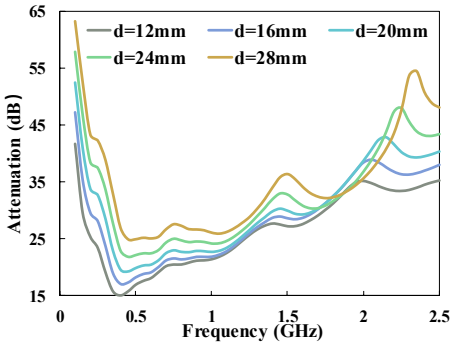

Fig. 15 Effect of rebar diameter on the signal attenuation

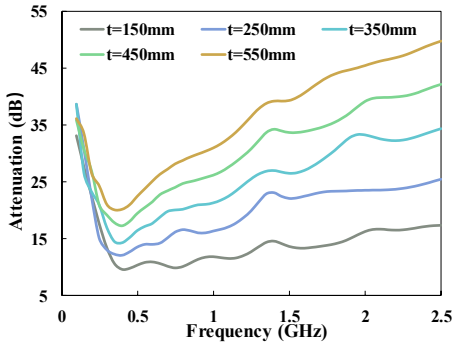

Fig. 16 Effect of slab thickness on the signal attenuation

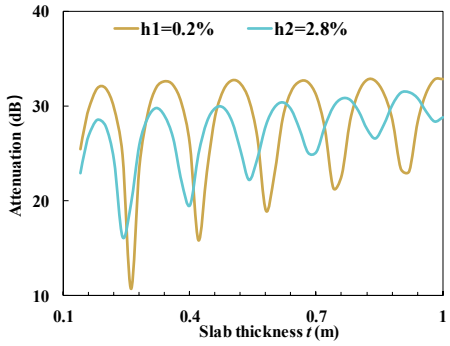

(a) Attenuation vs. slab thickness t

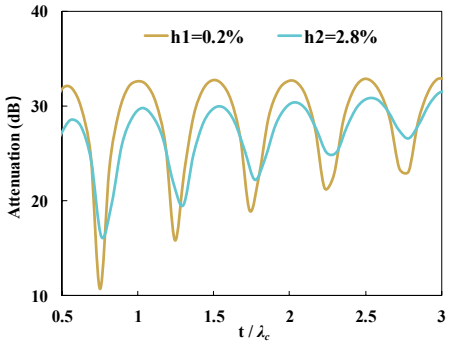

(b) Attenuation vs. t/λ_c

Fig. 17 Signal attenuation through reinforced concrete slab with low VWC at 433 MHz; g = 100 mm, d = 28 mm

Effect of thickness on signal attenuation through reinforced concrete slab is shown in Fig. 16. The simulation parameters are as follows: concrete VWC h_5 = 9.3%, d = 10 mm, g = 100 mm, and slab thickness t is variated in the range of 150 ~ 550 mm. Optimal frequency for different thickness slab is in the range of 0.38 ~ 0.40 GHz. That is, $f_{optimal}$ is barely influenced by slab thickness t. However, the minimum attenuation $L_{p,min}$ is linear with slab thickness t. $L_{p,min}$ = 9.7 dB for t = 150 mm, $L_{p,min}$ = 12.2 dB for t = 250 mm, $L_{p,min}$ = 14.3 dB for t = 350 mm, $L_{p,min}$ = 17.3 dB for t = 450 mm, $L_{p,min}$ = 20.2 dB for t = 550 mm. Signal attenuation increases 2.6 dB on average at $f_{optimal}$ with every 100 mm increase of t. Attenuation is barely influenced by slab thickness if $f < f_{optimal}$ as attenuation by steel rebar lattice is predominant. Influence of slab thickness is obviously increasing with the enlargement of f, because ttenuation by concrete absorption is predominant in the total attenuation and effect of steel rebar lattice is decreasing with increase of frequency.

All the four factors concrete VWC, steel rebar lattice period g, rebar diameter and slab thickness have been investigated above. Concrete VWC is found to be the most influential factor to signal attenuation through reinforced concrete structure. Concrete VWC has an important effect on both optimal frequency $f_{optimal}$ and minimum attenuation $L_{p,min}$. Slab thickness t has little effect on $f_{optimal}$ while has a significant effect on $L_{p,min}$. Steel rebar lattice period g and rebar diameter d has limited influence on both $f_{optimal}$ and $L_{p,min}$. Overall, $f_{optimal}$ lies in the range of 0.35 ~ 0.5 GHz considering all the four factors.

Based on the optimal frequency range for transmission through reinforced concrete structure, 433 MHz is chosen for the following attenuation simulation. The choice of 433 MHz has two reasons. One reason is that 433 MHz lies in the optimal range of 0.35 ~ 0.5 GHz as discovered above. More importantly, 433 MHz frequency range is allowed for wireless communication and has been gradually used for wireless underground sensor network (WUSN). The antenna size is 17 cm for wireless sensor node at this frequency, which can be acceptable for engineering application.

3.5 Attenuation analysis at 433 MHz through reinforced concrete slab

A further study is needed for attenuation analysis of signal transmission through reinforced concrete structures at 433 MHz. The most unfavorable parameters are used for the following simulation. Steel rebar lattice is maintained as 100 mm and rebar diameter is maintained as 28 mm. Effect of slab thickness t and concrete VWC are focus as they are the two most influential factors. Signal attenuation with different slab thickness is shown in Fig. 17(a) at low concrete VWC h_1 and h_2. It can be observed that signal attenuation has several resonant points. The resonant frequency is affected by concrete VWC. The local maximum of attenuation is barely affected by slab thickness while the local minimum of attenuation is highly sensitive to slab thickness. The local minimum increases with the enlargement of slab thickness. This reveals that the attenuation caused by concrete is gradually predominant in

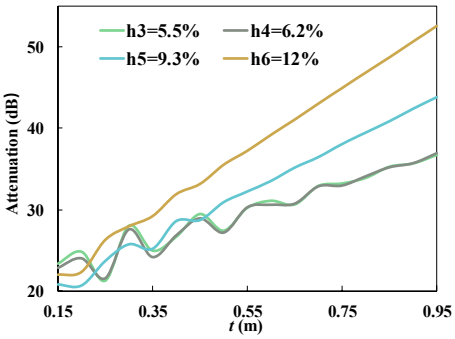

Fig. 18 Signal attenuation through reinforced concrete slab with high VWC at 433 MHz; g = 100 mm, d = 28 mm.

the total attenuation. Similar to the discussion for pure rebar lattice attenuation, thickness relative to wavelength in concrete t/λ_c is discussed instead of thickness. λ_c is 324 mm for concrete VWC at h_1 = 0.2%, and λ_c is 296 mm for concrete VWC at h_2 = 2.8%. Therefore, signal attenuation versus t/λ_c is obtained in Fig. 17(b). It is observed that resonant occurs at $t/(\lambda_c/4) = 2n$ and $t/(\lambda_c/4) = 2n+1$, n = 1, 2, 3, 4, …… Local maximum for attenuation occurs at $t/(\lambda_c/4) = 2n$ and local minimum occurs at $t/(\lambda_c/4) = 2n + 1$. This resonant phenomenon is identical with that of pure steel rebar lattice. It figures out that reinforced concrete slab behaves more like pure steel rebar lattice at low concrete VWC, and attenuation caused by steel rebar is predominant in the total attenuation. The difference lies at the local minimum attenuation which is increasing with slab thickness.

Signal attenuation at 433 MHz with high concrete VWC is given in Fig. 18. Different from low concrete VWC, signal resonance is not obvious at high concrete VWC and gradually vanishes with the increase of slab thickness. This can be explained that the increase of imaginary part of dielectric constant with concrete VWC promotes the energy absorption by concrete. In other words, the predominance of total attenuation is transformed from steel rebar reflection to concrete absorption at high concrete VWC. The relationship between signal attenuation and slab thickness gradually becomes linear. This linearity is more obvious for concrete VWC at h_5 = 9.3% and h_6 = 12%. Regression analysis gives the linear regression function: $L_p = 29.354\ t + 16.025$ with goodness of fit $R^2 = 0.9945$ for h_5 = 9.3%, $L_p = 38.721\ t + 15.935$ with $R^2 = 0.9981$ for h_6 = 12%.

4. Experiment verification for signal attenuation at 433 MHz

From what has been discussed, signal attenuation of transmitting through reinforced concrete structure has been simulated at 433 MHz. However, the previous experiment study has not covered 433 MHz in the frequency range of 0.5 GHz~2.0 GHz. Hence, the simulation signal attenuation transmitting plain concrete and reinforced concrete structures has to be validated by experiment at 433 MHz. Experiment setup is shown in Fig. 19. A two layers of wireless sensor network was adopted for signal attenuation test. This network consisted of two wireless sensors operating at 433 MHz and one gateway. Wireless sensor Node 1 was buried in a plain concrete slab and Node 2 was placed in the air. Wireless signal was transmitted from Node 1 and received by Node 2, and the wireless communication information was recorded by the gateway. The received signal strength (RSS) could be obtained via the remote server. The two wireless sensor nodes and the test specimen were placed inside a plumbum box to minimize the influence of outside EM interference. Different transmission distance could be controlled by the number of specimen. Each specimen was fabricated with the dimension of 600 mm × 600 mm and the thickness was 50 mm for plain concrete specimen and 200 mm for reinforced concrete specimen.

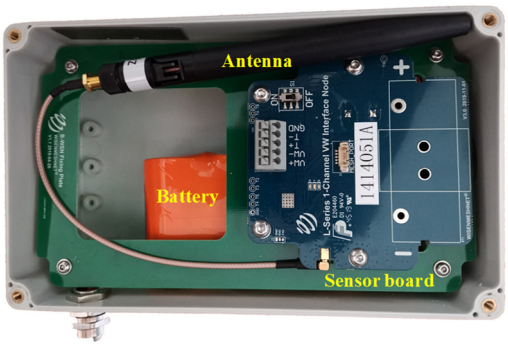

Fig. 20 Wireless interface node used in the signal attenuation test

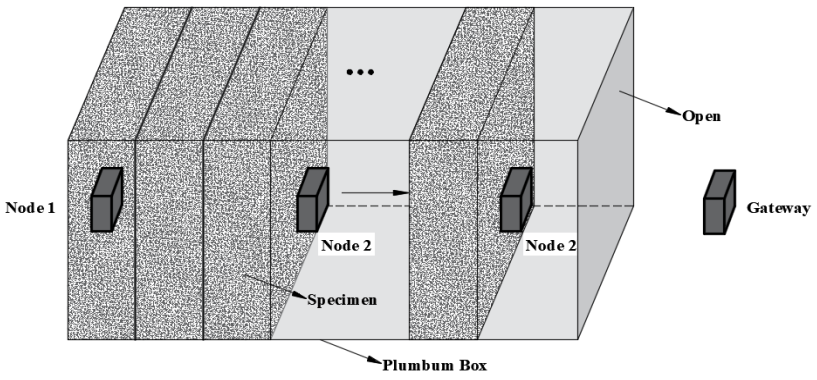

Fig. 19 Experimental setup for wireless signal attenuation test

(a) Reinforced concrete slab fabrication, steel rebar 25@50

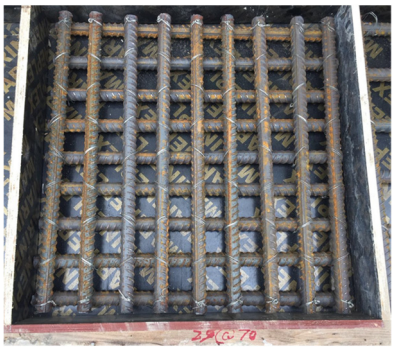

(b) Reinforced concrete slab fabrication, steel rebar 25@70

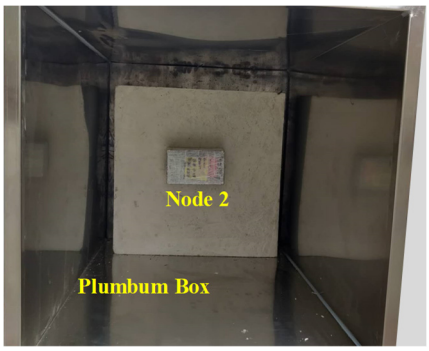

(c) Wireless signal attenuation test

Fig. 21 Specimen fabrication and signal attenuation test

The test system consisted of two wireless sensor nodes and one gateway. The wireless sensor node as shown in Fig. 20 was an interface node designed for the signal attenuation test. Two sensor nodes operated at 433 MHz and the antenna was placed inside the sensor box for protection. The antenna was vertically polarized, and the orientations of Node 1 and Node 2 were maintained the same throughout the whole experiment. Besides, each sensor node contained industrial typed D Cell batteries as power source, power management module and a MCU chip. At each time interval, sensor nodes formed a mesh topology and sent data to the gateway. The wireless protocol (namely, WISENMESHNET®) used in this experiment was designed specifically for a WSN monitoring system. It was based on EEE802.15.4. The gateway was responsible for the command issuing (such as T, F modifications) and data collection from all the nodes involved in a mesh network; meanwhile, it forwarded the data and system information to the remote server via mobile network.

Specimen fabrication was shown in Figs. 21(a) and (b) as an example. Node 1 was buried in a plain concrete slab and 11 more plain concrete slabs were fabricated to test the signal attenuation through different thickness concrete slab. For reinforced concrete slabs, four groups of steel rebar period (g = 50 mm, 70 mm, 100 mm, 150 mm) given rebar diameter at 25 mm were fabricated. Four specimens of RC slab were labeled as 25@50, 25@70, 25@100, 25@150. Single layer of steel rebar was centered in the 200 mm thick slab.

The experiment scenario was shown in Fig. 21(c). Specimen with Node 1 was placed at the bottom of the plumbum box, and the tested specimen was put between Node 1 and Node 2. The test protocol was as follows: Step 1, no specimen between Node 1 and Node 2, recorded the RSS of Node 2 as a baseline measurement; Step 2, specimen attenuation test, placed the specimen between Node 1 and Node 2 and recorded the RSS. The RSS difference between Step 1 and Step 2 was the attenuation of the tested specimen. Baseline measurement of Step 1 was designed to reduce the influence of complex signal propagation mechanism of antenna. Each RSS measurement was repeated for ten times to ensure the reliability.

Plain concrete attenuation test result and the comparison with finite element simulation was given in Fig. 22. The concrete dielectric permittivity was set as VWC = 5.5% for Jonscher model given in Table 2. Fig. 22 shows a good greement between test result and finite element simulation at 433 MHz for plain concrete slab. The maximum difference

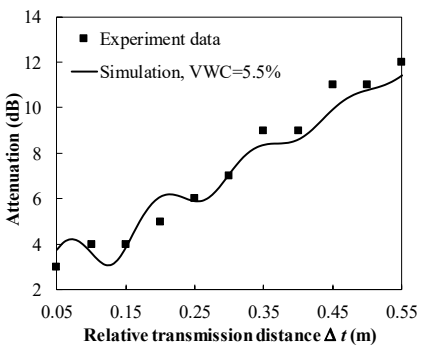

Fig. 22 Comparison of attenuation between experiment result and finite element simulation for plain concrete slab at 433 MHz

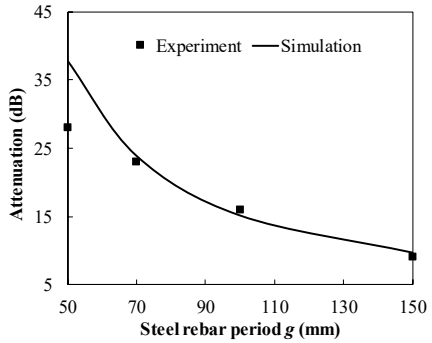

Fig. 23 Comparison of attenuation between experiment result and HFSS simulation for RC structure at 433 MHz

is 1.08 dB, Root Mean Squared Error (RMSE) is 0.60 dB and good of fit $R^2 = 0.96$.

Test results of reinforced concrete slab attenuation are illustrated in Fig. 23. The reinforced concrete slab was 200 mm thick and the experiment focused on the effect of steel rebar period on signal attenuation. The concrete VWC of reinforced concrete slab is still 5.5%, same as plain concrete slab. Fig. 23 shows that simulation has a very good fitness to the large steel rebar condition. The inconsistence happens at the very small steel rebar period g = 50 mm. The attenuation predicted by simulation is 9.9 dB higher than measured in the test. Consequently, applicability of finite element simulation for rebar period g smaller than 70 mm should be investigated by more experiments. FEM simulation is still applicable because g is seldom smaller than 70 mm for general civil engineering structures.

5. Conclusions

This paper simulates the attenuation for wireless signal transmission through plain concrete slab, pure steel rebar lattice and reinforced concrete slab in the frequency range of 0.1~2.5 GHz. Several conclusions are arrived as follows:

- Two kinds of concrete dielectric model, Jonscher model and Debye model, are used to fit attenuation test results. FEM simulation with Jonscher model has a good agreement with test results, and the maximum deviation is 0.41 dB~0.63 dB. FEM simulation with Debye model has a maximum deviation of 2.38 dB~3.49 dB from the test results. Jonscher model is a better dielectric model in characterizing the concrete permittivity.
- Attenuation for signal transmission through steel rebar lattice is dependent on frequency f, lattice period g, rebar diameter d and layer distance D between the two rebar layers. Signal attenuation for single layer steel rebar is controlled by g/λ. Signal attenuates a lot if $g/\lambda < 0.5$, and signal has very little attenuation if $g/\lambda \geq 0.5$. For signal transmission through two layers of rebar lattice, resonance occurs at $D/(\lambda/4) = 2n$, n = 1, 2, 3, … for local minimum and at $D/(\lambda/4) \approx 2n - 1$, n = 1, 2, 3, … for local maximum of attenuation.
- Attenuation for signal transmission through reinforced concrete slab is determined by concrete VWC, steel rebar lattice period g, rebar diameter d and slab thickness t. Concrete VWC is found to be the most influential factor to signal attenuation. Concrete VWC has an important effect on both optimal frequency $f_{optimal}$ and minimum attenuation $L_{p,min}$. Slab thickness t has little effect on $f_{optimal}$ while has a significant effect on $L_{p,min}$. Steel rebar lattice period g and rebar diameter d has limited influence on both $f_{optimal}$ and $L_{p,min}$. Overall, $f_{optimal}$ lies in the range of 0.35~0.5 GHz considering all the four factors.
- For signal transmission through RC slab, resonance occurs at $t/(\lambda_c/4) = 2n$ and $t/(\lambda_c/4) = 2n + 1$, n = 1, 2, 3, 4, … for low concrete VWC. Reinforced concrete slab behaves more like pure steel rebar lattice at low concrete VWC and attenuation caused by rebar reflection is predominant. Resonances gradually vanishes with the increase of slab thickness and concrete VWC. Signal attenuation is highly linear with slab thickness t for concrete VWC at h_5 = 9.3% and h_6 = 12%. The predominance is replaced by concrete absorption in the total attenuation for high concrete VWC.
- Optimal frequency is set as 433 MHz considering the optimization result and antenna size for wireless sensor network application. FEM simulation of signal attenuation through concrete and reinforced concrete slab at 433 MHz is verified by the experiment result.

Acknowledgments

This research was funded by the National Key R&D Program of China (Grant No. 2018YFC0704800), National Natural Science Foundation of China (No. 51978530, 52022070), Shanghai Science and Technology Committee (18DZ1201200).

References

Akyildiz, I.F., Su, W., Sankarasubramaniam, Y. and Cayirci, E. (2002), "Wireless sensor networks: a survey", *Comput. Netw.*, **38**(4), 393-422. https://doi.org/10.1016/S1389-1286(01)00302-4

Benatia, M.A., Louis, A., Baudry, D., Mazari, B. and El-Hami, A. (2014), "Impact of Radio Propagation in Buildings on WSN's Lifetime", *Proceedings of Global Summit on Computer and Information Technology* (*GSCIT*), New York, June.

Bennett, P.J., Soga, K., Wassell, I., Fidler, P., Abe, K., Kobayashi, Y. and Vanicek, M. (2010), "Wireless sensor networks for underground railway applications: case studies in Prague and London", *Smart Struct. Syst., Int. J.*, **6**(5-6), 619-639. https://doi.org/10.12989/sss.2010.6.5_6.619

Biaz, S., Yiming, J., Bing, Q. and Shaoen, W. (2005), "Dynamic signal strength estimates for indoor wireless communications", *Proceedings of International Conference on Wireless Communications, Networking and Mobile Computing*, Wuhan, China, September, pp. 602-605. https://doi.org/10.1109/WCNM.2005.1544117

Bourdi, T., Rhazi, J.E., Boone, F. and Ballivy, G. (2008),

"Application of Jonscher model for the characterization of the dielectric permittivity of concrete", *J. Phys. D: Appl. Phys.*, **41**(20), 205410. https://doi.org/10.1088/0022-3727/41/20/205410

Cendes, Z. (2016), "The development of HFSS", In: *2016 USNC-URSI Radio Science Meeting*, Fajardo, PR, USA, June, pp. 39-40. https://doi.org/10.1109/USNC-URSI.2016.7588501

Ceylan, H., Gopalakrishnan, K., Kim, S., Taylor, P.C., Prokudin, M. and Buss, A.F. (2013), "Highway Infrastructure Health Monitoring Using Micro-Electromechanical Sensors And Systems (Mems)", *J. Civil Eng. Manage.*, **19**(S), S188-S201. https://doi.org/10.3846/13923730.2013.801894

Chung, K.L., Yuan, L., Ji, S.T., Sun, L., Qu, C.P. and Zhang, C.W. (2017), "Dielectric characterization of Chinese standard concrete for compressive strength evaluation", *Appl. Sci.-Basel*, **7**(2), 14. https://doi.org/10.3390/app7020177

Corr, D.G. (1967), "Solution of a periodic boundary-value problem by direct application of Floquet's theorem", *Electron. Lett.*, **3**(11), 483-485. https://doi.org/10.1049/el:19670382

Dalke, R.A., Holloway, C.L., McKenna, P., Johansson, M. and Ali, A.S. (2000), "Effects of reinforced concrete structures on RF communications", *IEEE Transact. Electromag. Compatib.*, **42**(4), 486-496. https://doi.org/10.1109/15.902318

Dehmollaian, M. and Sarabandi, K. (2008), "An approximate solution of scattering from reinforced concrete walls", *IEEE Transact. Antennas Propag.*, **56**(8), 2681-2690. https://doi.org/10.1109/TAP.2008.927534

Deng, Y.J., Zhou, Z.X., Zhao, Z.D., Luo, Y., Yi, X.M., Li, J., Hui, G.H., Gao, Y.Y. and Shi, D.S. (2019), "Simulation Study on ASCMP Protocol in Utility Tunnel WSN", *IEEE Access*, **7**, 168141-168150. https://doi.org/10.1109/access.2019.2954182

Flanigan, K.A., Johnson, N.R., Hou, R., Ettouney, M. and Lynch, J.P. (2017), "Utilization of Wireless Structural Health Monitoring as Decision Making Tools for a Condition and Reliability-Based Assessment of Railroad Bridges", *Proceedings of Sensors and Smart Structures Technologies for Civil, Mechanical, and Aerospace Systems 2017*, Portland, OR, USA, March. https://doi.org/10.1117/12.2262933

Georgakopoulos, S.V. and Shan, J. (2010), "Wireless powering of sensors embedded in concrete", *Proceedings of 2010 IEEE 11th Annual Wireless and Microwave Technology Conference* (*WAMICON*), Melbourne, FL, USA, April, pp. 1-5. https://doi.org/10.1109/WAMICON.2010.5461866

Haque, M.E., Zain, M.F.M., Hannan, M.A. and Rahman, M.H. (2015), "Building structural health monitoring using dense and sparse topology wireless sensor network", *Smart Struct. Syst., Int. J.*, **16**(4), 607-621. https://doi.org/10.12989/sss.2015.16.4.607

Huang, H.W., Xie, X., Zhang, D.M., Liu, Z.Q. and Lacasse, S. (2019), "Multi-sensor data fusion based assessment on shield tunnel safety", *Smart Struct. Syst., Int. J.*, **24**(6), 693-707. https://doi.org/10.12989/sss.2019.24.6.693

Jiang, S. (2011), "Optimum wireless power transmission for sensors embedded in concrete", Ph.D. Dissertation; Florida International University, MI, USA.

Jiang, S. and Georgakopoulos, S.V. (2011), "Optimum wireless power transmission from air to lossy media", *WAMICON 2011 Conference Proceedings*, Clearwater Beach, FL, USA, April. https://doi.org/10.1109/WAMICON.2011.5872881

Jiang, S., Georgakopoulos, S.V. and Jin, H. (2012), "Effects of periodic reinforced-concrete structures on power transmission", *Proceedings of 2012 IEEE International Conference on RFID* (*RFID*), Orlando, FL, USA, April. https://doi.org/10.1109/RFID.2012.6193046

Jo, B.W., Park, J.H. and Yoon, K.W. (2013a), "The Experimental Study on Concrete Permeability of Wireless Communication Module Embedded in Reinforced Concrete Structures", *Int. J. Distrib. Sensor Networks*, **9**(6), 520507. https://doi.org/10.1155/2013/520507

Jo, H., Park, J.W., Spencer, B.F. and Jung, H.J. (2013b), "Develoment of high-sensitivity wireless strain sensor for structural health monitoring", *Smart Struct. Syst., Int. J.*, **11**(5), 477-496. https://doi.org/10.12989/sss.2013.11.5.477

Li, X., Ji, Z., Zhu, H. and Gu, C. (2012), "A feasibility study of the measuring accuracy and capability of wireless sensor networks in tunnel monitoring", *Front. Struct. Civil Eng.*, **6**(2), 111-120. https://doi.org/10.1007/s11709-012-0150-1

Lin, C., Kuo, L. and Chuang, H. (2006), "A horizontally polarized omnidirectional printed antenna for WLAN applications", *IEEE Transact. Antennas Propag.*, **54**(11), 3551-3556. https://doi.org/10.1109/TAP.2006.884307

Linderman, L.E., Rice, J.A., Barot, S., Spencer, B.F. and Bernhard, J.T. (2010), "Characterization of wireless smart sensor performance", *J. Eng. Mech.*, **136**(12), 1435-1443. https://doi.org/10.1061/(ASCE)EM.1943-7889.0000187

Liu, R.S., Wu, Y., Wassell, I. and Soga, K. (2009), "Frequency diversity measurements at 2.4 GHz for wireless sensor networks deployed in tunnels", *Proceedings of 2009 IEEE 20th International Symposium on Personal, Indoor and Mobile Radio Communications*, Tokyo, Japan, September. https://doi.org/10.1109/PIMRC.2009.5449796

Liu, R.S., Wassell, I.J. and Soga, K. (2010), "Relay node placement for wireless sensor networks deployed in tunnels", *Proceedings of 2010 IEEE 6th International Conference on Wireless and Mobile Computing, Networking and Communications*, Niagara Falls, ON, Canada, October. https://doi.org/10.1109/WIMOB.2010.5644984

Lott, M. and Forkel, I. (2001), "A multi-wall-and-floor model for indoor radio propagation", *IEEE VTS 53rd Vehicular Technology Conference*, Rhodes, May.

Luo, K., Ge, S., Zhang, L., Liu, H. and Xing, J. (2019), "Simulation Analysis of Ansys HFSS and CST Microwave Studio for Frequency Selective Surface", *Proceedings of 2019 International Conference on Microwave and Millimeter Wave Technology* (*ICMMT*), Guangzhou, China, May. https://doi.org/10.1109/VETECS.2001.944886

Lynch, J.P. (2007), "An overview of wireless structural health monitoring for civil structures", *Philos. Trans. R. Soc. A-Math. Phys. Eng. Sci.*, **365**(1851), 345-372. https://doi.org/10.1098/rsta.2006.1932

Micheli, D., Delfini, A., Santoni, F., Volpini, F. and Marchetti, M. (2015), "Measurement of electromagnetic field attenuation by building walls in the mobile phone and satellite navigation frequency bands", *IEEE Antennas Wireless Propag. Lett.*, **14**, 698-702. https://doi.org/10.1109/LAWP.2014.2376811

Nagayama, T., Sim, S.H., Miyamori, Y. and Spencer, B.F. (2007), "Issues in structural health monitoring employing smart sensors", *Smart Struct. Syst., Int. J.*, **3**(3), 299-320. https://doi.org/10.12989/sss.2007.3.3.299

Nagayama, T., Spencer, B.F. and Rice, J.A. (2009), "Autonomous decentralized structural health monitoring using smart sensors", *Struct. Control Health Monitor.*, **16**(7-8), 842-859. https://doi.org/10.1002/stc.352

Ou, J., Li, H. and Yu, Y. (2004), "Development and performance of wireless sensor network for structural health monitoring", *Proceedings of SPIE 5391, Smart Structures and Materials 2004: Sensors and Smart Structures Technologies for Civil, Mechanical, and Aerospace Systems*, San Diego, CA, USA, July. https://doi.org/10.1117/12.540812

Pathmanathan, P., Jones, C.M., Pytel, S.G., Edgar, D.L. and Huray, P.G. (2011), "Power loss due to periodic structures in high-speed packages and Printed Circuit Boards", *Proceedings of the 18th European Microelectronics & Packaging Conference*, Brighton, UK, September.

Raju, K.S., Pratap, Y., Sahni, Y. and Babu, M.N. (2015), "Implementation of a WSN system towards SHM of civil building structures", *Proceedings of 2015 IEEE 9th International Conference on Intelligent Systems and Control*, Coimbatore, India, January. https://doi.org/10.1109/ISCO.2015.7282303

Sandrolini, L., Reggiani, U. and Ogunsola, A. (2007), "Modelling the electrical properties of concrete for shielding effectiveness prediction", *J. Phys. D: Appl. Phys.*, **40**(17), 5366-5372. https://doi.org/10.1088/0022-3727/40/17/053

Soutsos, M.N., Bungey, J.H., Millard, S.G., Shaw, M.R. and Patterson, A. (2001), "Dielectric properties of concrete and their influence on radar testing", *NDT & E International*, **34**(6), 419-425. https://doi.org/10.1016/S0963-8695(01)00009-3

Stone, W.C. (1997), "Electromagnetic signal attenuation in construction materials", *NIST Interagency/Internal Report (NISTIR) No. 6055, United States Department of Commerce Technology Administration National Institute of Standards and Technology*. https://doi.org/10.6028/NIST.IR.6055

Sundaram, B.A., Ravisankar, K., Senthil, R. and Parivallal, S. (2013), "Wireless sensors for structural health monitoring and damage detection techniques", *Current Sci.*, **104**(11), 1496-1505. https://doi.org/10.1038/srep01962

Wu, D., Bao, L.C. and Li, R.F. (2010), "A holistic approach to wireless sensor network routing in underground tunnel environments", *Comput. Commun.*, **33**(13), 1566-1573. https://doi.org/10.1016/j.comcom.2010.04.017

Zhou, Z.X., Shao, C.N., Zheng, H.N., Zhou, H.M., Yang, X., Lou, X.W., Li, J., Hui, G.H. and Zhao, Z.D. (2020), "Simulating study on RHCRP protocol in utility tunnel WSN", *Wirel. Netw.*, **26**(4), 2797-2808. https://doi.org/10.1007/s11276-019-02038-y